Plant Physiology Increases the Magnitude and Spread of the Transient Climate Response to CO₂ in CMIP6 Earth System Models

CLAIRE M. ZARAKAS

Department of Atmospheric Sciences, University of Washington, Seattle, Washington

ABIGAIL L. S. SWANN

Department of Atmospheric Sciences, and Department of Biology, University of Washington, Seattle, Washington

MARYSA M. LAGUË

Department of Atmospheric Sciences, University of Washington, Seattle, Washington, and Department of Earth and Planetary Science, University of California, Berkeley, Berkeley, California

KYLE C. ARMOUR

Department of Atmospheric Sciences, and School of Oceanography, University of Washington, Seattle, Washington

JAMES T. RANDERSON

Department of Earth System Science, University of California, Irvine, Irvine, California

(Manuscript received 5 February 2020, in final form 23 May 2020)

ABSTRACT

Increasing concentrations of CO_2 in the atmosphere influence climate both through CO_2 's role as a greenhouse gas and through its impact on plants. Plants respond to atmospheric CO_2 concentrations in several ways that can alter surface energy and water fluxes and thus surface climate, including changes in stomatal conductance, water use, and canopy leaf area. These plant physiological responses are already embedded in most Earth system models, and a robust literature demonstrates that they can affect global-scale temperature. However, the physiological contribution to transient warming has yet to be assessed systematically in Earth system models. Here this gap is addressed using carbon cycle simulations from phases 5 and 6 of the Coupled Model Intercomparison Project (CMIP) to isolate the radiative and physiological contributions to the transient climate response (TCR), which is defined as the change in globally averaged near-surface air temperature during the 20-yr window centered on the time of CO_2 doubling relative to preindustrial CO_2 concentrations. In CMIP6 models, the physiological effect contributes $0.12^{\circ}C$ (σ : $0.09^{\circ}C$; range: $0.02^{\circ}-0.29^{\circ}C$) of warming to the TCR, corresponding to 6.1% of the full TCR (σ : 3.8%; range: 1.4%-13.9%). Moreover, variation in the physiological contribution to the TCR across models contributes disproportionately more to the intermodel spread of TCR estimates than it does to the mean. The largest contribution of plant physiology to CO_2 -forced warming—and the intermodel spread in warming—occurs over land, especially in forested regions.

1. Introduction

Increasing concentrations of atmospheric CO₂ alter global temperature both through CO₂'s role as a greenhouse gas

© Supplemental information related to this paper is available at the Journals Online website: https://doi.org/10.1175/JCLI-D-20-0078.s1.

Corresponding author: Claire M. Zarakas, czarakas@uw.edu

within the atmosphere (radiative effect) and through plants' response to CO₂ at the land surface (physiological effect). Plants respond to atmospheric CO₂ concentrations by regulating their stomata (pores on the leaves that modulate the exchange of CO₂ and water vapor between the leaf and the atmosphere), changing water use, adjusting canopy leaf area, and, ultimately, changing species composition and vegetation cover. These plant physiological responses to higher CO₂ can physically influence land surface temperature by

altering land evapotranspiration, surface albedo, and surface roughness, which are important controls over the fluxes of water and energy between the land surface and the atmosphere. Here we use the term "physiological effect" to encompass the net biogeophysical effect of all plant responses to increasing CO₂, but note that in some previous studies (e.g., Skinner et al. 2018) the term refers solely to the effect of changes in stomatal conductance. The physiological effect in this study may therefore be smaller than some previous estimates (e.g., Skinner et al. 2018; Cao et al. 2010) because increases in leaf area can counteract the influence of changes in stomatal conductance on land evapotranspiration.

Plant responses to CO₂ modulate land evapotranspiration through two opposing mechanisms. Higher concentrations of CO₂ in the atmosphere provide a larger gradient over which CO2 diffuses into the interior airspace of leaves. As a result, most plant types close their stomata in response to increasing CO₂, thereby decreasing transpiration per unit of leaf area (Field et al. 1995). In contrast, photosynthetic rates under some environmental conditions are limited by access to CO₂, and in these instances more CO₂ can lead to higher rates of photosynthesis, which is often referred to as CO₂ fertilization. CO₂ fertilization tends either to have no influence on canopy leaf area or to increase canopy leaf area (Norby and Zak 2011; Donohue et al. 2013), which increases transpiration. The physiological effect's net influence on land evapotranspiration therefore depends on the relative magnitude of the stomatal response and the leaf area response, as well as the extent to which vegetation influences land-atmosphere interactions in a given region (Lian et al. 2018). Most Earth system models (ESMs; Swann et al. 2016; Lemordant et al. 2018) and field experiments (Hungate et al. 2002; Leakey et al. 2009) suggest that the stomatal response term dominates in areas with moderate to high leaf area, leading to a net decrease in land evapotranspiration. However, future projections of photosynthetic rates, leaf growth rates, and thus transpiration remain highly uncertain (Friedlingstein et al. 2006; Anav et al. 2013; Piao et al. 2013; Smith et al. 2016; Lian et al. 2018).

Physiologically driven reductions in evapotranspiration can warm local land temperatures directly by decreasing evaporative cooling, as well as indirectly through influences on low-level humidity, cloud cover, and precipitation. Recent modeling studies have demonstrated that physiologically driven decreases in land evapotranspiration can reduce cloud cover by decreasing low-level relative humidity (Doutriaux-Boucher et al. 2009; Andrews et al. 2011, 2012; de Arellano et al. 2012; Lemordant et al. 2018), which amplifies regional physiologically driven warming. If the leaf area response were to dominate over

stomatal responses, the resulting increase in evapotranspiration could decrease land temperatures through these same mechanisms. Physiologically forced drying of the boundary layer and warming of the land surface can also impact large-scale atmospheric dynamics and regional precipitation (Kooperman et al. 2018a; Langenbrunner et al. 2019; Saint-Lu et al. 2019; Park et al. 2020).

In addition to influencing land surface temperature by altering evapotranspiration, the plant physiological response to CO₂ can also influence land surface temperature by altering land surface albedo. CO₂ fertilization generally decreases albedo (thereby increasing temperature) by increasing leaf area and, within dynamic vegetation models, by shifting plant functional types from grasses to trees (Bala et al. 2006; Andrews et al. 2019). Expansion of forests in boreal and Arctic regions can result in especially large albedo decreases (Betts 2000; Bala et al. 2006; O'ishi et al. 2009; Andrews et al. 2019; Xu et al. 2020) because increases in foliage mask bright snow.

The global-scale temperature implications of plants' physiological responses to CO2 have been long acknowledged. Sellers et al. (1996) were the first to quantify physiologically driven warming by coupling a biosphere model to an atmosphere model, finding that under a doubling of CO₂ the physiological effect increased global land temperature by about 0.3°C and mean global temperature by about 0.1°C. Since then, multiple modeling studies have demonstrated that the plant physiological response tends to increase land temperature in most modern ESMs on annual time scales (Betts et al. 2007; Cao et al. 2010; Andrews et al. 2011; Arora et al. 2013; Swann et al. 2016; Lemordant et al. 2016, 2018; Arora et al. 2019) and during heatwaves (Lemordant et al. 2016; Skinner et al. 2018; Lemordant and Gentine 2019). In particular, as part of their analysis to disentangle carbon-concentration and carbon-climate feedbacks, Arora et al. (2013, 2019) show that the physiological effect drives modest transient global warming in most ESMs from phases 5 (Arora et al. 2013; Figs. 2a-c) and 6 (Arora et al. 2019; Figs. 4a-c) of the Coupled Model Intercomparison Project (CMIP5 and CMIP6, respectively), although they explicitly quantify the physiological warming only for the multimodel mean.

Despite this demonstrated physiological influence on global surface temperatures, the physiological effect has received limited recognition in the climate dynamics literature. Although plants' physiological responses to CO₂ are already embedded in many ESMs that are used to estimate the transient climate response (TCR) and equilibrium climate sensitivity (ECS), studies that explicitly quantify the physiological contribution to such global-scale climate sensitivity metrics have been limited

TABLE 1. Summary of CMIP experiments used.

			Influence of CO ₂ concentration on		
Experiment	CMIP5 experiment name	CMIP6 experiment name	Land	Ocean	Atmosphere
FULL	1pctCO2	1pctCO2	1% per year	1% per year	1% per year
PHYS	esmFixClim1	1pctCO2-bgc	1% per year	1% per year	Pre-industrial
RAD	exmFdbk1	1pctCO2-rad	Pre-industrial	Pre-industrial	1% per year
PI	piControl	piControl	Pre-industrial	Pre-industrial	Pre-industrial

to ESMs from a few individual modeling centers (summarized in Table S1 in the online supplemental material; Sellers et al. 1996; Betts et al. 1997; Cox et al. 1999; Douville et al. 2000; Levis et al. 2000; Bala et al. 2006; Betts et al. 2007; Doutriaux-Boucher et al. 2009; Boucher et al. 2009; Cao et al. 2009; O'ishi et al. 2009; Cao et al. 2010; Andrews et al. 2011; Pu and Dickinson 2012). Physiology's contribution to the TCR has not been systematically assessed across models and CMIP phases.

Additionally, past studies in the climate sensitivity literature have not specifically quantified the physiological contribution to the TCR using the same experimental methodology from which the full TCR is calculated. For example, baseline levels of CO₂ have ranged from 280 to 400 ppm across experiments (Table S1) and the physiological effect's influence on temperature has been analyzed from both abrupt (Doutriaux-Boucher et al. 2009; Cao et al. 2010; Andrews et al. 2011) and transient (Bala et al. 2006; Boucher et al. 2009) CO₂ perturbations. Modeling studies have also differed in whether they include both the stomatal and leaf area components of the physiological effect or only the stomatal component. While these different experimental designs have provided insights into the mechanisms and time scales of the physiological effect's influence on climate, they do not provide systematic estimates of the full physiological contribution to the TCR across ESMs.

The lack of systematic intermodel comparison of the physiological contribution to the TCR is a problematic gap in the existing literature because past work suggests that physiologically driven warming differs across models. Arora et al. (2013, 2019) documented that the magnitude of global physiologically driven warming varies across models, reflecting that models differ both in how plants respond to increasing CO₂ (Friedlingstein et al. 2006; Anav et al. 2013; Piao et al. 2013; Smith et al. 2016; Lian et al. 2018) and in how the atmosphere responds to perturbations to the land surface energy budget (Andrews et al. 2009; Devaraju et al. 2018). This suggests that intermodel disagreement about the magnitude of physiologically driven warming may be an unrecognized contributor to intermodel spread in CO2-forced warming. Additionally, poor model agreement on the magnitude of physiologically driven warming would mean that an estimate derived from a single model may not capture the true multimodel mean. To address this gap, we use standardized carbon cycle model simulations from the CMIP5 and CMIP6 archives to assess 1) the magnitude of the physiological effect's influence on temperature across models, 2) whether trends in the physiological effect contribute to the increase in the TCR noted for many recent models (Andrews et al. 2019; Golaz et al. 2019; Flynn and Mauritsen 2020), 3) the spatial pattern of physiologically driven temperature changes, 4) how physiological processes contribute to variability in multimodel estimates of the TCR, and 5) the mechanisms through which the physiological effect influences temperature.

2. Methods

a. CMIP experiments

As part of CMIP5 and CMIP6, modeling groups performed three concentration-driven experiments (summarized in Table 1) in which CO₂ concentrations increase by 1% per year from preindustrial levels (284.3 ppm) to a quadrupling of CO₂ (1144.9 ppm), while all other forcings remain at preindustrial levels. The spatial pattern of vegetation in these simulations comes from the preindustrial era; this spatial pattern remains constant throughout the simulation except for in land models with dynamic vegetation (Tables S2 and S3), where the distribution of plant functional types changes based on climate and resource availability. In one set of simulations, referred to here as FULL (CMIP6 experiment "1pctCO2"), both the atmosphere and carbon cycle (on land and in the oceans) experience increasing CO₂ concentrations. Additional experiments conducted as part of the Coupled Climate-Carbon Cycle Model Intercomparison Project (C4MIP; Friedlingstein et al. 2006; Jones et al. 2016) enable us to isolate how much the physiological and radiative effects of CO₂ each contribute to surface warming. In a set of C4MIP simulations, referred to here as RAD (CMIP6 experiment "1pctCO2-rad"), only the atmosphere experiences increasing CO₂ concentrations, while the terrestrial and oceanic carbon cycles experience constant preindustrial CO₂ concentrations. In another set of C4MIP simulations, referred to here as PHYS (CMIP6 experiment "1pctCO2-bgc"), the radiative transfer submodels in the atmosphere experience constant preindustrial CO₂ concentrations, while the land surface and ocean carbon cycle submodels experience the increasing CO₂ concentrations. We use the concentration-driven preindustrial control experiment (referred to here as PI; CMIP6 experiment "piControl") as the baseline from which anomalies are calculated.

b. Models

We analyze output from all ESMs that had uploaded near-surface air temperature monthly data for the FULL, PI, and PHYS and/or RAD experiment to the Earth System Grid by 13 May 2020. This consisted of 8 CMIP5 models (Table S2) and 12 CMIP6 models (Table S3). These models all include interactive representations of the carbon cycle; plants in these models respond to increasing CO₂ by changing leaf area, stomatal conductance, and, in some models, the location and distribution of plant functional types (indicated in Tables S2 and S3). Three models from CMIP6 have dynamic vegetation; however, we do not believe this is a large enough set of models to draw general conclusions about the impact of dynamic vegetation. In addition, one of these three models is UKESM1-0-LL, which has a significantly larger physiologically driven temperature response relative to other models, but it is unclear if this stronger temperature response is driven by dynamic vegetation.

Ocean responses to increasing CO_2 include changes in inorganic and biological carbon cycling, which have negligible direct influences on modeled ocean surface temperature. The only potential direct influences of ocean carbon cycle responses on ocean surface temperatures in the PHYS experiments are through changes in plankton community structure, which can alter 1) ocean biogeophysical properties and 2) the emission of gases and particles, which influence aerosol formation (Hense et al. 2017). These effects are not represented in most models. We calculate multimodel mean maps after regridding model output to a consistent 0.9424° latitude \times 1.25° longitude grid.

c. Calculation of climate sensitivity metrics TCR and T140

We calculate the TCR as the change in globally averaged near-surface air temperature during the 20-yr window centered on the time of CO₂ doubling (years 61–80 of the simulation where CO₂ concentration increases by 1% per year) relative to preindustrial atmospheric CO₂ concentration. When using the PI experiment as a control, we account for model drift by subtracting the

Forster (2008), where year 1–140 following Gregory and Which FULL, RAD, and PHYS were branched from PI. We refer to the physiological and radiative contributions to the full TCR as TCR_{PHYS} and TCR_{RAD}, respectively.

We also quantify the physiological and radiative contributions to the T140 metric (Gregory et al. 2015; Grose et al. 2018). We calculate T140 as the change in globally averaged near-surface air temperature during the 20-yr window that ends at the time of CO₂ quadrupling (years 121–140 of the simulation where CO₂ concentration increases by 1% per year) relative to the linearly detrended PI experiment following Gregory et al. (2015).

We assess whether our estimates of physiologically driven warming are robust relative to variability in the Earth system by comparing TCR_{PHYS} and T140_{PHYS} to the distribution of 20-yr running mean global temperatures in the full PI control experiments (Fig. S1). In two of the CMIP6 models evaluated here (BCC-CSM2-MR and CNRM-ESM2-1), large multidecadal (greater than 20 years) oscillations exist in the PI control (Fig. S1; noted in Parsons et al. 2020). The magnitude of these oscillations greatly exceeds the magnitude of the TCR_{PHYS} signal, and thus we cannot confidently quantify TCR_{PHYS} for these two models. These models' large multidecadal PI oscillations also have implications for TCR_{FULL}, as they suggest that model TCR_{FULL} estimates may be strongly influenced by variability rather than only representing the CO₂-forced warming signal, since for these models smoothing out variability would require an averaging period of greater than 20 years.

d. Isolating physiology's influence on temperature

We quantify the influence of the physiological effect in two ways: as the difference between the FULL and RAD simulations (FULL-RAD) and as the difference between the PHYS and PI simulations (PHYS-PI). Both represent physiology's influence on the TCR, but FULL-RAD includes any nonlinear interactions between the radiative and physiological effects of increasing CO₂, while PHYS-PI does not. For example, FULL-RAD would include the interaction between CO₂ fertilization and changes in leaf area [quantified as the leaf area index (LAI)] induced by radiatively driven warming. Warming generally increases vegetation productivity in high latitudes that are temperature-limited under current conditions (Qian et al. 2010), thereby increasing leaf area (Keenan and Riley 2018), while some ESMs suggest warming may decrease vegetation productivity and leaf area in the tropics (Mahowald et al. 2016) where current temperatures are already near plants' optimal temperatures for photosynthesis. We focus on the FULL-RAD methodology in the main text

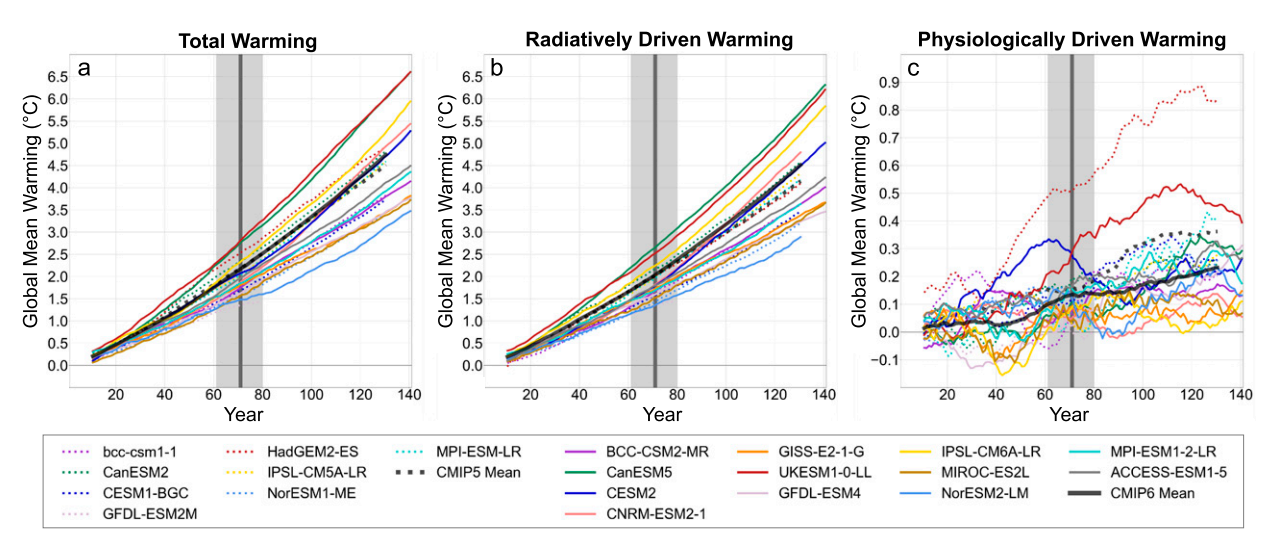


FIG. 1. Time series of global mean temperature change for (a) all CO_2 -forced warming, as calculated from FULL-PI; (b) the radiative contribution to global mean CO_2 -forced warming, as calculated from RAD-PI; and (c) the physiological contribution to global mean CO_2 -forced warming, as calculated from FULL-RAD. Time series in (a), (b), and (c) are smoothed with a 20-yr rolling average. The dark gray vertical line marks the time of CO_2 doubling, and the light gray bar indicates the 20-yr period surrounding the time of CO_2 doubling. Colors indicate modeling center and line types indicate CMIP phase (CMIP5: dashed; CMIP6: solid). Temperature changes for GFDL-ESM2M are only shown for years 1–80 because this model stopped ramping up CO_2 concentration after reaching $2xCO_2$. Note that the set of models included in the average differs between CMIP5 and CMIP6, and that the y-axis scale in (c) differs from (a) and (b).

because it emphasizes how much the physiological effect changes climate relative to what models would otherwise show from radiative forcing alone. Because FULL and RAD branch from the same point of the PI simulation, using FULL-RAD to quantify the physiological effect also avoids issues related to drift in the PI control. We discuss the nonlinearity between the radiative and physiological effects of CO₂ in more detail in the supplemental material (Note S1; Figs. S2–S5).

e. Partitioning physiological influences on evapotranspiration

To partition the total physiologically driven change in land evapotranspiration into its component physiological drivers, we derived Eq. (1) (see Derivation S1 in the supplemental material). The four terms on the right-hand side of Eq. (1) indicate the land evapotranspiration change due to 1) changes in leaf area, 2) changes in stomatal conductance (approximated as changes in transpiration per leaf area), 3) interactions between changes in stomatal conductance and changes in leaf area, and 4) changes in land evaporation:

$$\Delta \text{ET} = \left(\frac{T}{L}\right)_{\text{RFF}} \Delta L + L_{\text{RFF}} \Delta \frac{T}{L} + \Delta \frac{T}{L} \Delta L + \Delta E, \quad (1)$$

where ET is evapotranspiration (mm day⁻¹), T is transpiration (mm day⁻¹), L is leaf area index (unitless), and E is evaporation (mm day⁻¹). The REF subscript indicates the value from the reference experiment without

physiological responses to CO_2 (RAD for the FULL-RAD method and PI for the PHYS-PI method), and Δ indicates the physiologically driven change (e.g., as calculated from FULL-RAD).

3. Results

a. Physiology's contribution to the TCR and T140

The radiative effect of CO₂ is, unsurprisingly, the dominant contributor to both the TCR and T140. However, we also find that the physiological response to increased CO₂ makes a nonnegligible secondary contribution to the TCR and T140 in many CMIP5 and CMIP6 models (Figs. 1 and 2). In CMIP6 models, the physiological effect contributes about 0.12°C (σ: 0.09°C; range: 0.02°– 0.29°C) to the TCR, corresponding to 6.1% of the full TCR (σ : 3.8%; range: 1.4%–13.9%) (Table 2). For a few CMIP6 models (especially UKESM1-0-LL and CESM2), the physiological contribution to warming is quite large, accounting for over 10% of the full TCR (Table 2). Physiologically driven warming increases with increasing CO₂ concentration (Fig. 1c), on average contributing 0.21° C (σ : 0.12° C; range: 0.03° – 0.45° C) to the T140 metric (Table S4). On a percentage basis, the physiological effect contributes proportionally less to the T140 metric (4.9%; σ : 2.5%) than to the TCR, although this varies across models (Table S4).

In CMIP5 models, the physiological effect contributes 0.14° C (σ : 0.16° C; range: 0.00° – 0.51° C) to the TCR,

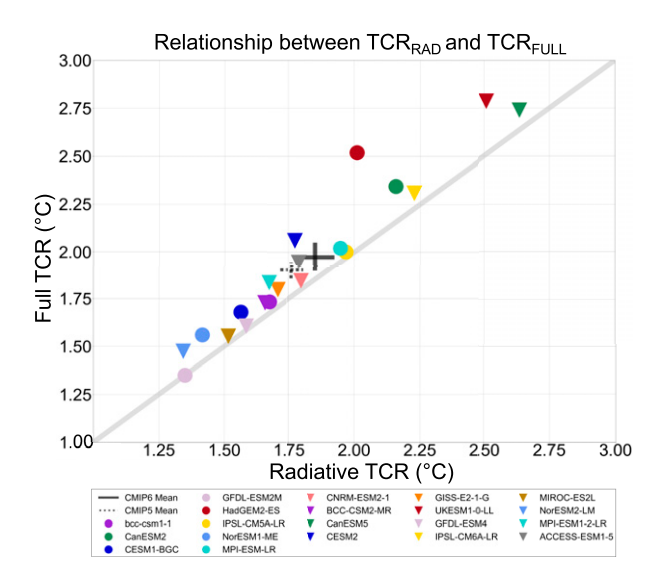


FIG. 2. The relationship between TCR_{RAD} (RAD-PI) and TCR_{FULL} (FULL-PI). The gray 1:1 line is where we would expect all models to be if the TCR were entirely caused by the radiative effects of CO_2 . The added warming from the physiological effect is the vertical distance between the gray 1:1 line and each point. Marker types indicate CMIP phase (CMIP5: circles; CMIP6: triangles) and colors indicate modeling center. Crosses demarcate the CMIP6 (solid) and CMIP5 (dashed) multimodel means, and the width of each cross corresponds to two times the ensemble mean standard deviation in global mean near-surface temperature from the preindustrial control.

corresponding to 6.6% of the full TCR (σ : 6.3%; range: 0.1%–20.1%). When comparing the same subset of eight models for which we have model output from both CMIP phases, physiologically driven warming is comparable in CMIP5 and CMIP6 (Table 2). This suggests that the increases in TCR_{FULL} from CMIP5 to CMIP6 noted for many recent models (Andrews et al. 2019; Golaz et al. 2019; Flynn and Mauritsen 2020) were driven primarily by increases in TCR_{RAD} rather than TCR_{PHYS}.

The multimodel mean TCR_{PHYS} values reported here are within the range of estimates from other studies (summarized in Table S1) but on the low side of this range, likely for two reasons. First, many previous studies isolated the effect of the stomatal response on near-surface temperatures rather than the net effect of both the stomatal and leaf area responses to increasing CO₂ (Table S1); we expect a larger temperature increase from the stomatal response alone than from the combined stomatal and leaf area responses because increases in leaf area counteract the stomatal response's influence on evapotranspiration. Second, our study is the first to compare TCR_{PHYS} across models (12 from CMIP6 and 8 from CMIP5), and the fact that the existing literature did not capture the full spread in

TCR_{PHYS} across models underscores the importance of a multimodel approach.

The global mean TCR_{PHYS} signal is small in comparison to TCR_{FULL}, and it is statistically significant relative to the preindustrial control for only 7 of 12 CMIP6 and 5 of 8 CMIP5 models at 2xCO₂ (Table S5). By 4xCO₂, the physiologically driven warming signal emerges from the noise for more models (Fig. S1), becoming statistically significant for 9 CMIP6 and 7 CMIP5 models (Table S5). The three CMIP6 models that are not statistically significant by 4xCO₂ (CNRM-ESM2-1, BCC-CSM2-MR, and IPSL-CM6A-LR) are the three models with the most variability in the PI control of all the CMIP5 and CMIP6 models we analyze (Fig. S1).

b. Spatial pattern of physiologically driven warming

The physiological effect only directly influences land surface properties, and thus the largest warming driven by the physiological effect occurs over land. In CMIP6 models, the physiological effect results in nonglaciated land warming by 0.22°C at 2xCO₂ and 0.41°C at 4xCO₂ on average, relative to a corresponding mean ocean warming of 0.09° and 0.14°C respectively (Fig. 3a). Physiologically driven warming over land is also statistically significant for more ESMs than it is for the global mean at both 2xCO₂ and 4xCO₂ (Table S5). The spatial pattern of physiologically driven warming that we find is consistent with other studies, which also show the greatest warming over land and modest ocean warming (Table S1).

The greatest mean physiologically driven warming occurs over boreal forests and nonglaciated highlatitude land, followed by temperate and tropical forested regions. The agreement across models is reasonably high—at least 8 of 12 CMIP6 models agree that the physiological effect results in warming in these three biomes at 2xCO₂ (Fig. S4) and 10 of 12 CMIP6 models show warming in these biomes at $4xCO_2$ (Fig. S5). Relative to radiatively driven warming, physiology also contributes more to land warming than ocean warming, with physiological forcing constituting a mean 7.4% of total CO₂-forced land warming at 2xCO₂ compared to 4.5% of ocean warming (Fig. 3b). The physiological effect therefore amplifies the land-ocean warming contrast: at 4xCO₂ nonglaciated land warms faster than the ocean with a mean ratio of 1.60 for the RAD simulations from CMIP6, whereas the mean land-ocean warming contrast for the FULL simulations is 1.64, due to the addition of the physiological effect (Fig. 4). This physiologically driven enhancement of the land-ocean warming contrast was previously demonstrated for Met Office Hadley Centre models (Joshi et al. 2008;

TABLE 2. TCR_{FULL}, TCR_{RAD}, and TCR_{PHYS} by model, where TCR_{PHYS} is calculated by both PHYS-PI and FULL-RAD. The consistent model subset refers to the models for which the necessary model output is available for both CMIP5 and CMIP6. For the summary statistics in the last four rows, the percentages refer to the mean and standard deviations of the percent contributions across models.

		CMI	P5 mo	CMIP5 model TCR	~					CMI	P6 mo	CMIP6 model TCR				
							FU	FULL-							FU	FULL-
		FULL		RAD	PHYS-PI	S-PI	Κ.	RAD		FULL		RAD	PHYS-PI	S-PI	Z	RAD
Modeling center	Model name	ွ	ပ	%	္	%	ွ	%	Model name	ွ	ပ္	%	ွင	%	ပ္	%
Beijing Climate	BCC-CSM1-1	1.73	1.67	%5.96	0.05	2.8%	90.0	3.5%	BCC-CSM2-MR	1.73	1.66	95.8%	0.54	31.4%	0.07	4.2%
Canadian Centre for Climate Modeling and	Can ESM2	2.34	2.16	92.1%	0.15	6.5%	0.19	7.9%	Can ESM5	2.74	2.64	96.2%	0.04	1.5%	0.10	3.8%
Analysis (CCCma) National Center for Atmospheric	CESM1-BGC	1.68	1.56	93.2%	0.11	%9.9	0.11	%8.9	CESM2	2.06	1.78	86.1%	0.11	5.2%	0.29	13.9%
Research (NCAR) NOAA Geophysical Fluid Dynamics	GFDL-ESM2M	1.35	1.35	%6.66	0.05	3.4%	0.00	0.1%	GFDL-ESM4	1.61	1.58	%9.86	0.17	10.7%	0.02	1.4%
Laboratory (NOAA-GFDL) Met Office Hadley	HadGEM2-ES	2.52	2.01	79.9%	0.37	14.6%	0.51	20.1%	UKESM1-0-LL	2.79	2.51	%0.06	0.17	%0.9	0.28	10.0%
Institut Pierre Simon	IPSL-CM5A-LR	2.00	1.97	98.3%	0.11	5.6%	0.03	1.7%	IPSL-CM6A-LR	2.31	2.23	96.4%	0.17	7.3%	0.08	3.6%
Laplace (IFSL) Norwegian Climate	NorESM1-ME	1.56	1.42	%8.06	0.08	5.3%	0.14	9.2%	NorESM2-LM	1.48	1.34	91.0%	1	I	0.13	%0.6
Max Planck Institute for	MPI-ESM-LR	2.02	1.95	96.4%	0.20	%6.6	0.07	3.6%	MPI-ESM1-2-LR	1.84	1.67	91.1%	0.13	7.2%	0.16	8.9%
Commonwealth Scientific and Industrial	I	1	I	I	I	I	1	I	ACCESS-ESM1–5	1.95	1.79	91.9%	0.21	10.7%	0.16	8.1%
Research Organization (CSIRO) Centre National de Recherches	I	I	1	I	I	I	I	I	CNRM-ESM2-1	1.84	1.80	. %5".26	-0.15	-8.0%	0.05	2.5%
Météorologiques (CNRM-CERFACS) NASA Goddard Institute for Space Studies	I	1		1	1	1	1	1	GISS-E2-1-G	1.80	1.71	94.9%	0.08	4.3%	0.09	5.1%
(NASA-GISS) Japan Agency for Marine- Earth Science and Technology (JAMSTEC)	I	I		I	l	I	I	I	MIROC-ES2L	1.55	1.52	%9'.26	0.07	4.8%	0.04	2.4%
Mean	All models Consistent model subset	1.90	1.76	93.4%	0.14%	6.8%	0.14	%9·9 %9·9	All models Consistent model subset	1.97	1.85	93.9%	0.14	7.4%	0.12	6.1%
Standard deviation	All models Consistent model subset	0.40	0.30	6.3%	0.11	3.8% 4.1%		6.3%		0.43	0.40	3.8% 4.2%	0.16	9.4% 9.9%	0.09	3.8% 4.2%

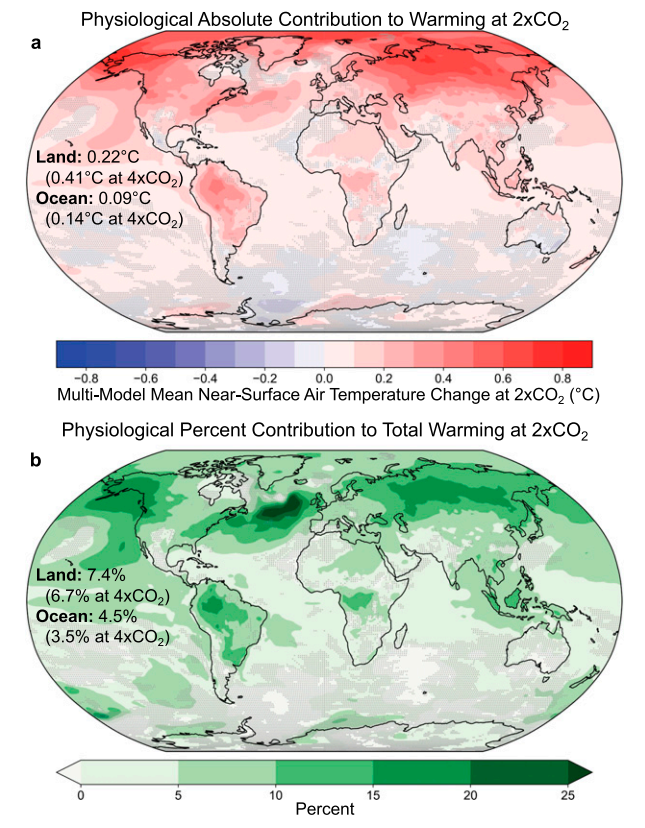


FIG. 3. Spatial pattern of (a) absolute physiologically driven warming and (b) physiological percent contribution to total warming at 2xCO₂, where physiologically driven warming is calculated by FULL-RAD. Multimodel means include the 12 CMIP6 models. Stippling indicates regions where less than 8 out of the 12 models agree on the sign of change.

Dong et al. 2009), and we show here that this warming contrast is robust across most CMIP models. In two models the physiological effect reduces the land—ocean warming contrast (Fig. 4). These outliers may result from large leaf area increases counteracting the influence of stomatal closure on evapotranspiration (resulting in minimal net physiologically driven change in evapotranspiration; Fig. S7) or from large multidecadal variability in some models (Fig. S1) overwhelming the physiological signal.

The larger absolute and relative physiologically driven warming over nonglaciated land is consistent with the physiological effect directly influencing land surface properties in regions with plant cover, while influencing glaciated land and oceans only indirectly through changes in heat transport, clouds, and other aspects of climate dynamics. Although the remote influence of physiological forcing on oceans and glaciated land is relatively modest, most models agree that the

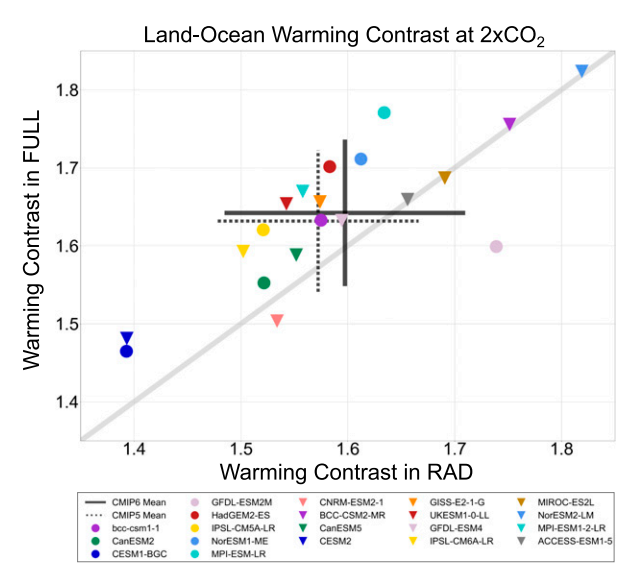


FIG. 4. The relationship between the land-ocean warming contrast (the ratio of the change in mean nonglaciated land near-surface air temperature to the change in mean ocean near-surface air temperature) from RAD (RAD-PI) and FULL (FULL-PI) at 2xCO₂. The gray 1:1 line is where we would expect all models to be if the warming contrast were entirely caused by the radiative effects of CO₂. Physiology's addition to the warming contrast is the vertical distance between the gray 1:1 line and each point. Marker types indicate CMIP phase (CMIP5: circles; CMIP6: triangles) and colors indicate modeling center as in Fig. 2. Crosses demarcate multimodel means, where the width of each cross is two standard deviations across models. Note that the set of models included in the average differs between CMIP5 and CMIP6.

physiological effect results in mean warming of nearsurface oceanic air and ocean surface layers. The regions of the most robust physiologically driven oceanic warming across models are the western North Atlantic, equatorial Pacific, equatorial Indian Ocean, and highlatitude Pacific.

Byrne and O'Gorman (2018) suggest that increases in the near-surface land-ocean temperature contrast are causally driven by temperature change over the ocean. However, the physiologically driven enhanced landocean contrast, where the only initial difference is over the land surface, shows that land surface processes can also initiate the feedback loop where decreasing relative humidity over land leads to a larger increase in temperature over land relative to over ocean. The potential to initiate this loop through land processes is noted by Byrne and O'Gorman (2016), and we further emphasize that point here. It is important to acknowledge the physiological effect's greater relative contribution to land warming because land warming (rather than global mean warming) is the most relevant metric for many societal climate impacts.

TABLE 3. Drivers of intermodel spread in global mean warming, as quantified by the standard deviation. "Land" specifically means nonglaciated land.

		$2xCO_2$ (TCR)		4xCO ₂ (T140)	
CMIP phase	Region	FULL-PI	RAD-PI	FULL-PI	RAD-PI
CMIP6	Global	0.43°C	0.40°C (92%)	1.02°C	0.98°C (96%)
	Land	0.58°C	0.50°C (86%)	1.32°C	1.19°C (90%)
	Ocean	0.38°C	0.36°C (95%)	0.91°C	0.90°C (99%)
CMIP5	Global	0.40°C	0.30°C (76%)	1.09°C	0.95°C (87%)
	Land	0.58°C	0.39°C (68%)	1.55°C	1.24°C (80%)
	Ocean	0.33°C	0.27°C (81%)	0.91°C	0.84°C (91%)

c. Physiology's contribution to uncertainty in CO_2 -forced warming

The magnitude of global physiologically driven warming varies significantly across models (Figs. 1 and 2; see also Fig. S6) and this uncertainty contributes to the intermodel spread of TCR estimates. In the CMIP6 models analyzed here, the radiative effect alone explains about 91.9% of the standard deviation in the TCR across models (Table 3), with the physiological effect contributing the remaining 8.1%. Thus, the impact of the physiological effect on model-to-model variability is disproportionately large relative to its contribution to the mean (8.1% for the standard deviation versus 6.1% for the mean). The physiological effect accounts for relatively less intermodel spread in the T140 metric (Table 3), consistent with other work (Geoffroy et al. 2012, Lutsko and Popp 2019) demonstrating that radiative feedbacks contribute increasingly more to intermodel disagreement in warming with increasing time in the transient 1pctCO₂ experiment.

The physiological effect contributes more to uncertainty in CO₂-forced warming over land. Averaged across all nonglaciated land, the physiological effect explains about 13.6% of the standard deviation in mean land warming across models at 2xCO₂ in CMIP6 (Table 3). In some highly forested land regions (tropical Africa, northwestern South America, and the southeastern United States), intermodel disagreement in local warming at 2xCO₂ is driven by approximately equal contributions of uncertainty from physiologically and radiatively forced warming (Fig. 5). These results suggest that the physiological effect is a nonnegligible contributor to intermodel spread in the TCR and regional land CO₂-forced warming at 2xCO₂. However, some of these preindustrial forested regions are largely deforested in the present day, which means that in scenario-based future projections the physiological effect may contribute less to uncertainty in these regions than Fig. 5 implies.

The physiological effect contributes less to uncertainty in CO₂-forced warming over the ocean, explaining about

5.1% of the standard deviation of the mean ocean warming across models at 2xCO₂ in CMIP6 (Table 3). In all oceanic regions, intermodel disagreement in CO₂-forced warming is driven more by radiative processes than the physiological effect (Fig. 5). However, Fig. 5 suggests that physiology is a significant secondary driver of intermodel disagreement in the magnitude of CO₂-forced warming in some ocean regions (e.g., North Atlantic and North Pacific), possibly due to intermodel disagreement in the extent to which physiological responses influence cloud cover in these regions [discussed in section 3d(2)].

d. Mechanisms of physiologically driven warming

1) MECHANISMS OVER LAND

The physiological effect increases near-surface air temperatures over land by modifying surface properties that modulate terrestrial energy fluxes (Bonan 2008;

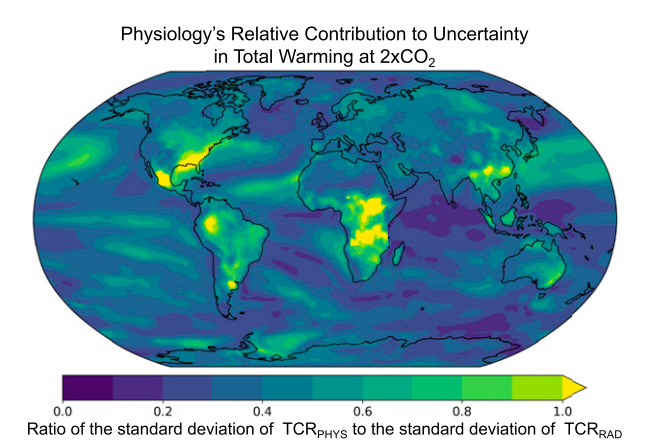


FIG. 5. Spatial pattern of physiology's relative contribution to intermodel spread in CO₂-forced warming, as quantified by the ratio of the standard deviation (σ ; at each grid cell, across models) of physiologically forced warming (calculated from FULL-RAD) to σ of radiatively forced warming (calculated from RAD-PI) at 2xCO₂ for CMIP6 models, i.e., $\sigma_{\rm PHYS}({\rm lat, lon})/\sigma_{\rm RAD}({\rm lat, lon})$. A value of 1 means that the physiological and radiative effects of CO₂ contribute equally to the total uncertainty in local warming at 2xCO₂ across models.

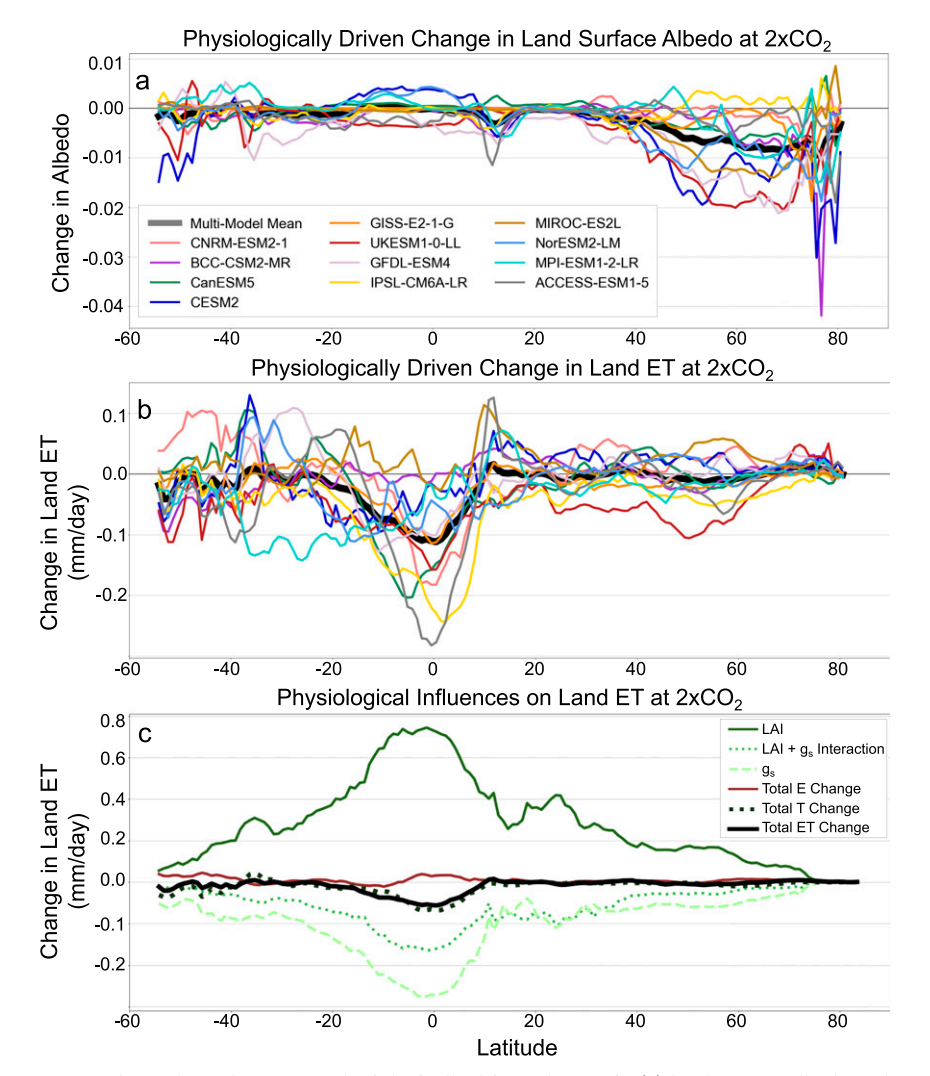


FIG. 6. Land zonal means of physiologically driven changes in (a) land surface albedo and (b) evapotranspiration at $2xCO_2$ for CMIP6 models, as calculated by FULL-RAD. (c) Zonal means of how much physiologically driven changes in different land processes (LAI, stomatal conductance g_s , and evaporation) contribute to the total multimodel mean physiologically driven change in land evapotranspiration, where the partitioning is calculated with Eq. (1). Multimodel means in this figure are averaged across all CMIP6 models for which model output is available. Transpiration and LAI data necessary for this partitioning were not available for GFDL-ESM4, MPI-ESM1.2-LR, and ACCESS-ESM1.5 so these models are only included in the multimodel mean for the total evapotranspiration change.

Laguë et al. 2019). This occurs through 1) changes in the partitioning between surface turbulent fluxes resulting from physiological influences on evapotranspiration, 2) radiative changes due to physiologically driven changes in albedo, cloud cover, and column water vapor, and 3) changes in surface roughness resulting from changes in leaf area and vegetation distribution.

In most models, plants' response to CO₂ causes a net decrease in mean land evapotranspiration, especially in

the tropics (Fig. 6 and Fig. S7), indicating that stomatal closure decreases evapotranspiration by enough to offset increases in evapotranspiration from increased leaf area, though the magnitude and sign of evapotranspiration change does vary spatially across models (Fig. S7). In the CMIP6 multimodel mean at $2xCO_2$, global leaf area changes increase land evapotranspiration by $0.19 \, \text{mm day}^{-1}$ (σ : $0.17 \, \text{mm day}^{-1}$; range: 0.00– $0.52 \, \text{mm day}^{-1}$), changes in stomatal conductance (approximated by the change in transpiration per leaf area)

FIG. 7. Spatial pattern of multimodel mean physiologically driven changes in surface energy fluxes as calculated by FULL-RAD at the point of CO_2 doubling (averaged over years 61–80) for (a) clear-sky downwelling shortwave radiation, (b) cloudy downwelling shortwave radiation, (c) upwelling shortwave radiation, (d) net shortwave radiation, (e) clear-sky downwelling longwave radiation, (f) cloudy downwelling longwave radiation, (g) upwelling longwave radiation, (h) net longwave radiation, (i) latent heat (LH), (j) sensible heat (SH), (k) heat uptake (G), and (l) net radiation ($R_{\rm net}$). Because the surface energy budget is balanced, LH + SH + $G = R_{\rm net}$. The cloudy radiative fluxes in (b) and (f) are calculated as the difference between all-sky and clear-sky radiative fluxes. Multimodel means include all CMIP6 models for which model output is available; this consists of up to 12 models. Data for some surface energy fluxes were not available for the following models: GFDL-ESM4 [in (a), (b), (e), and (f)], GISS-E2.1-G [in (j) and (k)], and NorESM2-LM [in (e) and (f)]. Stippling indicates regions where fewer than eight models agree on the sign of change.

decrease global land evapotranspiration by 0.13 mm day⁻¹ $(\sigma: 0.10 \,\mathrm{mm} \,\mathrm{day}^{-1}; \,\mathrm{range}: 0.00-0.29 \,\mathrm{mm} \,\mathrm{day}^{-1}), \,\mathrm{and}$ the interaction between changes in stomatal conductance and leaf area decreases evapotranspiration by an additional 0.08 mm day⁻¹ (σ : 0.10 mm day⁻¹; range: $0.00-0.29 \,\mathrm{mm}\,\mathrm{day}^{-1}$; Fig. 6c). Land evaporation changes minimally $(0.01 \text{ mm day}^{-1}; \sigma: 0.03 \text{ mm day}^{-1}; \text{ range:}$ from -0.06 to +0.06 mm day⁻¹; Fig. 6c). In the multimodel mean, the net effect of these physiological responses is a decrease in evapotranspiration, with the largest and most robust decrease in the tropics (Fig. 6; see also Fig. S7). This physiologically driven decrease in evapotranspiration due to increased CO₂ has previously been documented for CMIP5 models (Swann et al. 2016; Lemordant et al. 2018) and holds for the new CMIP6 models analyzed here. Under constant net radiation at the surface, this physiologically driven decrease in evapotranspiration results in more energy leaving the land surface through sensible heating (Fig. 7), thereby increasing near-surface air temperatures.

The physiological effect also increases surface and near-surface temperatures by generally increasing the net radiation at the surface. Net shortwave radiation on land increases primarily through decreases in albedo and cloud cover (Fig. 7d). Albedo decreases primarily in high latitudes (Fig. 6), due to both increases in leaf area and decreases in snow cover due to increased temperatures. Consistent with previous studies (Doutriaux-Boucher et al. 2009; Andrews et al. 2011, 2012; de Arellano et al. 2012; Lemordant et al. 2018), downwelling shortwave radiation (SW_{down}) reaching the surface also increases as a consequence of decreases in cloud cover (especially in the Northern Hemisphere middle and high latitudes and over the northeastern Amazon; Fig. 7b), which are driven both by decreases in relative humidity from physiologically forced reductions in evapotranspiration and by increases in air temperature. In the multimodel mean, the physiological effect causes only modest changes in clear-sky SW_{down} (Fig. 7), although some individual models do show significant SW_{down} changes, which could be modified by changes in water vapor and aerosols [e.g., as Andrews et al. (2012) documented in HadGEM2-ES due to vegetation's influence on dust optical depth].

The physiological effect also influences surface net longwave radiation (Fig. 7l) through changes in surface and boundary layer temperatures, cloud cover, atmospheric column water vapor, and the partitioning of surface energy fluxes. Outgoing longwave radiation from the land surface (LW_{up}) increases with increasing surface temperature through the Planck feedback (Fig. 7g). This increase in LW_{up} is partially offset by increases in clear-sky downward longwave radiation at the land surface (LW_{down}; Fig. 7e). Clear-sky LW_{down} increases due to warming of the boundary layer driven by both increased sensible heating and by longwave radiation associated with surface warming (Vargas Zeppetello et al. 2019), and clear-sky LW_{down} can also be influenced by physiologically driven changes in atmospheric water vapor. Cloud changes resulting from reduced land evapotranspiration decrease LW_{down} (Fig. 7f). The net effect of all of these processes generally results in a decrease of net longwave radiation over most vegetated land (Fig. 7h).

2) MECHANISMS OVER OCEAN

Because most models do not have any mechanism through which ocean carbon cycle responses to CO₂ can influence ocean temperatures, the modeled oceanic warming as calculated by FULL-RAD must be the result of remote, land-driven warming. Recognizing the oceanic component of physiologically driven warming is important because it constitutes about half of TCR_{PHYS}—even though the magnitude of physiologically driven oceanic warming is much smaller than land warming on a per area basis, the TCR is a global-scale metric and ocean constitutes about 70% of Earth's surface area.

The physiological effect on land can alter ocean temperatures through advection of continental air that has been directly influenced by changes in land surface properties (e.g., changes in air temperature or moisture content) as well as through changes in atmospheric or oceanic circulation. Some robust oceanic warming regions are downwind of warming land regions, which could be associated with advection of warm continental air by the prevailing winds. Cloud cover over oceans also decreases in some regions that are downwind of land, particularly in the North Atlantic, increasing ocean temperatures by increasing net radiation (Fig. 7). Teleconnections likely also contribute to ocean warming, based on past work indicating that changes in largescale atmospheric circulation and atmospheric energy transport can be induced by physiological forcing (Kooperman et al. 2018a; Langenbrunner et al. 2019; Saint-Lu et al. 2019; Park et al. 2020) or other changes in land surface properties (Swann et al. 2012, 2014; Devaraju et al. 2015; Laguë and Swann 2016; Devaraju et al. 2018). Additionally, the physiological effect has the potential to induce changes in ocean circulation (e.g., Diffenbaugh et al. 2004). Exploration of the links between land surface perturbations and ocean temperature merits further research.

4. Discussion and implications

a. Magnitude of the physiological contribution to the transient climate response

The biological and ecological processes governing canopy leaf area and stomatal conductance are often considered to exist squarely in the domain of carbon cycle feedbacks (i.e., they impact the climate system through their influence on CO₂ concentrations themselves). Our analysis demonstrates that these terrestrial carbon cycle processes are also embedded in global climate sensitivity metrics like the TCR through plants' impact on land surface properties and surface energy fluxes.

We quantified the plant physiological effect's small but significant influence on CO₂-forced temperature changes, finding that at 2xCO₂ the physiological effect contributes about 0.12°C (6.1%) to the TCR and leads to about 0.22°C of warming over nonglaciated land. Recognizing this physiological component of CO₂ forcing is necessary for understanding forcing differences across greenhouse gases (e.g., increasing N₂O concentration does not induce warming from physiological responses) and has implications for estimating the TCR from historical observations. Because some of the observed historical temperature change has been driven by non-CO₂ forcing agents that do not induce physiological responses in plants, estimates of the TCR from historical observations may be biased low, although this is likely a small effect since CO₂ currently constitutes the majority of the total radiative forcing. While the physiological effect can constitute over 10% of the total TCR in some CMIP6 models, changes in the representation of plant physiology do not appear to be a driver of the increase in the TCR observed from CMIP5 to CMIP6.

The significant physiologically driven warming at higher CO₂ concentrations, intermodel agreement in the sign of TCR_{PHYS}, and consistent spatial pattern of warming give us confidence that we are detecting a real physiologically driven signal and not just a residual from internal variability. However, internal variability is a large source of uncertainty in quantifying TCR_{PHYS} (Fig. 1c), and this uncertainty is intrinsically included in estimates of TCR_{FULL}. Integration of a large-ensembles approach into the next C4MIP is necessary to address this issue and to reduce uncertainties in the TCR in future work (Deser et al. 2020). This could be done by integrating a requirement for a minimum

number of initial condition ensembles in the experiment.

A limitation of our study is that the C4MIP model output necessary to disentangle physiologically and radiatively forced warming is only available for about a quarter of the models for which we can estimate the full TCR (12 of 47 for CMIP6 and 8 of 30 for CMIP5). We therefore cannot quantify TCR_{PHYS}, or the physiological contribution to uncertainty in the TCR, for the remaining CMIP models. Future work could further leverage C4MIP model output to assess whether signatures of physiologically driven warming (such as seasonal variations in the CO₂-forced change of the diurnal temperature range; Bounoua et al. 1999; Collatz et al. 2000) could be used to estimate the physiological contributions to mean warming from the FULL experiments alone.

b. Physiology's role in forcing, feedbacks, and equilibrium climate sensitivity

From the perspective of the classical radiative forcingfeedback framework (Gregory et al. 2004; Bony et al. 2006; Roe 2009; Boucher et al. 2013), plants' physiological response to increasing CO₂ can be considered a forcing—rather than a feedback—on the climate system because by definition plants are responding to changes in CO₂ rather than to the relatively slow changes in global temperature. The time scale over which plants respond to increasing CO₂ ranges from on the order of seconds to decades. The stomatal response is fast; at the leaf level, stomata respond to changing environmental conditions in less than an hour (Vico et al. 2011), and the time scale of the atmospheric adjustment to the stomatal response occurs on the time scale of a few months (Doutriaux-Boucher et al. 2009; Andrews et al. 2011). Doutriaux-Boucher et al. (2009) have demonstrated that this fast stomatal response rapidly reduces low cloud cover and thereby the cloud radiative effect, which has been shown to be an important contributor to global warming and its uncertainty (Geoffroy et al. 2012). The leaf area and plant distribution responses are slower, occurring on time scales of years to decades (Fisher et al. 2019).

Whether the physiological effect will be included in the calculation of radiative forcing depends on the definition used. The physiological effect would be excluded from the *instantaneous* radiative forcing, which accounts only for the instantaneous impact of CO₂ on the top-of-atmosphere radiation budget. However, it would be included in the *effective* radiative forcing, which is commonly expressed as a change in net top-of-atmosphere (TOA) radiation following CO₂-driven adjustments in tropospheric and stratospheric

temperatures, water vapor, clouds, and surface properties, prior to any global mean surface temperature change (e.g., Boucher et al. 2013; Sherwood et al. 2015). In practice, the effective radiative forcing is often calculated using simulations in which CO_2 is increased while sea surface temperatures (SSTs) are prescribed to be fixed at preindustrial values, with some studies estimating and removing the TOA radiative response to land warming when calculating the forcing value (Hansen et al. 2005; Vial et al. 2013; Tang et al. 2019). Meanwhile, radiative feedbacks are traditionally defined by the change in net TOA radiation for a given change in global mean surface temperature (Bony et al. 2006; Roe 2009).

The physiological response of plants to increasing CO₂ poses a challenge to this radiative forcing–feedback paradigm. On the one hand, plants respond directly to the atmospheric CO₂ concentration, suggesting that the physiological effect should be classified as part of the forcing. On the other hand, this direct physiological response of plants to CO₂ induces changes in surface temperature due to reduction in evaporative cooling from stomatal responses (even in the absence of the radiative effects of CO₂ changes). The TOA radiative response to these changes could thus be classified as part of the feedback within a framework that defines the effective radiative forcing as the TOA radiation change with fixed global mean temperature (e.g., Hansen et al. 2005). Meanwhile, temperature-driven changes in vegetation distribution and leaf area that influence land surface albedo and evapotranspiration should clearly be classified as feedbacks. While it is unclear to us how best to interpret the physiological effect in terms of the forcing-feedback paradigm, the distinction does not impact the results presented here because of our results' focus on the TCR instead of forcing or feedbacks separately.

Understanding of the role of the physiological effect in TCR and ECS uncertainty would benefit from greater clarity on whether it should be treated as a forcing or feedback. Indeed, recent work suggests that the TCR may be more sensitive to uncertainty in CO2 radiative forcing than to uncertainty in radiative feedbacks (Lutsko and Popp 2019), but that the ECS is more sensitive to uncertainty in radiative feedbacks (Geoffroy et al. 2012). Thus, while the results here suggest that the physiological effect will act to increase the ECS and its uncertainty-as it has for the TCR-we cannot currently quantify the magnitude of the effect on the ECS across models in the CMIP5 or CMIP6 ensembles. In this regard, it would be helpful if more modeling centers conducted additional radiation-only experiments for abrupt CO₂ quadrupling, using both coupled model simulations to be able to estimate ECS [e.g., as done for UKESM by Andrews et al. (2019)] and fixed SSTs¹ to be able to quantify the effective radiative forcing.

c. Broad implications of carbon cycle uncertainty

The terrestrial carbon cycle's influence on global temperature means that uncertainty in terrestrial carbon cycle processes contributes to uncertainty in CO₂-forced warming. We find that in CMIP6, the physiological effect explains about 13.6% of the standard deviation in CO₂-forced warming over nonglaciated land. We also identify several forested land regions (tropical Africa, northwestern South America, and the southeastern United States) for which the physiological effect contributes as much as the radiative effect (i.e., about 50% of the total) to intermodel disagreement in local warming at 2xCO₂. The spread in the magnitude of physiologically driven warming across CMIP6 models represents real scientific uncertainty, as there are limited observational constraints to suggest that either the high or low extremes of modeled physiological responses of stomatal conductance, leaf area, and resulting evapotranspiration are within expectations (Medlyn et al. 2011; De Kauwe et al. 2013; Schimel et al. 2015).

It is also possible that ESMs do not probe the full scientific uncertainty surrounding plants' responses to CO₂, as models may contain systematic biases. For example, many models represent stomatal conductance using the same key parameters [e.g., the same slope constant in the Ball-Berry stomatal conductance model (Ball et al. 1987) or the same g1 fitted parameter in the Medlyn et al. (2011) model] to govern how stomatal conductance responds to increasing CO₂, despite the wide variation in these parameters across and within plant functional types (Lin et al. 2015; Wolz et al. 2017). Similarly, some studies suggest (e.g., Smith et al. 2016) that ESMs systematically overestimate the leaf area increases resulting from CO2 fertilization, which would mean that models overestimate physiologically driven albedo decreases and underestimate physiologically driven evapotranspiration decreases. We would expect this to result in a true physiologically forced temperature change that is smaller than models suggest at high latitudes (where albedo matters more) and larger than models suggest at low latitudes (where ET matters more). Furthermore, Green et al. (2017) suggest that ESMs may systematically underestimate some feedbacks between land biosphere changes and the atmosphere.

On the one hand, acknowledging the physiological contribution to uncertainty in modeled CO2-forced warming suggests that models agree more on the magnitude of radiatively forced warming than the prevailing narrative implies. For atmospheric dynamicists most interested in purely radiatively driven processes, these findings therefore motivate more deliberate consideration of plant functioning in experimental designs; RAD simulations may be more appropriate than FULL simulations for some climate dynamics questions. On the other hand, acknowledging the physiological contribution means that reducing uncertainty in the full (Earth system) TCR requires reducing uncertainty in land surface processes which are especially difficult to constrain. From this perspective, these findings provide a new motivation for further experimental studies to reduce uncertainty in terrestrial carbon cycle processes. For example, we identify that plants' responses to CO₂ are a major driver of uncertainty in transient warming in tropical Africa, and no free-air CO₂ enrichment (FACE) experiments currently exist in tropical forests to constrain uncertainty in how those ecosystems will respond to increasing CO_2 .

Additionally, while this study focuses on how the physiological effect influences temperature and the TCR, uncertainty surrounding plant physiological responses to CO₂ can influence many aspects of the climate system. Because plant physiological responses affect land evapotranspiration, uncertainty surrounding plant physiological responses propagates to uncertainty in the hydrologic cycle. Previous studies have demonstrated that plant physiological responses play a critical role in determining the influence of increasing CO₂ concentration on runoff (Kooperman et al. 2018b) and precipitation (Kooperman et al. 2018a; Chadwick et al. 2017, 2019), especially in the Amazon (Richardson et al. 2018; Langenbrunner et al. 2019). Our finding that plant physiology contributes to intermodel variation in CO₂forced warming could therefore motivate further analyses of RAD and PHYS experiments to quantify the physiological contribution to uncertainty in these quantities. Carbon cycle uncertainty is not limited to the carbon cycle, and efforts to reduce uncertainty in plants' responses to CO₂ will also help to reduce uncertainty in the physical climate response to increasing CO_2 .

Acknowledgments. CMZ was supported by the University of Washington Program on Climate Change Fellowship and the Department of Energy Computational Science Graduate Fellowship (DE-SC0020347). MML was supported by the James S. McDonnell Foundation. ALSS,

¹ For example, the CMIP6 Cloud Feedback Model Intercomparison Project (CFMIP; Webb et al. 2017) tier 2 experiment piSST-4xCO2-rad, in which SSTs are fixed at preindustrial levels and only the radiation scheme (and not the vegetation scheme) experiences an abrupt quadrupling of CO₂.

MLL, and CMZ were supported by the National Science Foundation AGS-1553715 to the University of Washington. KCA was supported by the National Science Foundation AGS-1752796 to the University of Washington. JTR acknowledges support from the RUBISCO Scientific Focus Area that receives funding from the Regional and Global Modeling program within the Biological and Environmental Research division of DOE's Office of Science. We acknowledge the organizations responsible for CMIP, including the climate modeling groups that participated in C4MIP and shared their model output by uploading it to the Earth System Grid Federation.

Data availability statement. The majority of model output data used in this study are available in the publicly accessible Earth System Grid Federation (ESGF) repository at https://esgf-node.llnl.gov/projects/esgf-llnl/. Model output from the CESM2 RAD experiment is not yet available on the ESGF repository and is stored on data servers at the National Center for Atmospheric Research. The code used for this study is available from the corresponding author upon request.

REFERENCES

- Anav, A., and Coauthors, 2013: Evaluating the land and ocean components of the global carbon cycle in the CMIP5 Earth system models. J. Climate, 26, 6801–6843, https://doi.org/ 10.1175/JCLI-D-12-00417.1.
- Andrews, T., P. M. Forster, and J. M. Gregory, 2009: A surface energy perspective on climate change. *J. Climate*, 22, 2557– 2570, https://doi.org/10.1175/2008JCLI2759.1.
- ——, M. Doutriaux-Boucher, O. Boucher, and P. M. Forster, 2011: A regional and global analysis of carbon dioxide physiological forcing and its impact on climate. *Climate Dyn.*, 36, 783–792, https://doi.org/10.1007/s00382-010-0742-1.
- —, M. A. Ringer, M. Doutriaux-Boucher, M. J. Webb, and W. J. Collins, 2012: Sensitivity of an Earth system climate model to idealized radiative forcing. *Geophys. Res. Lett.*, 39, L10702, https://doi.org/10.1029/2012GL051942.
- —, and Coauthors, 2019: Forcings, feedbacks, and climate sensitivity in HadGEM3-GC3.1 and UKESM1. J. Adv. Model. Earth Syst., 11, 4377–4394, https://doi.org/10.1029/2019MS001866.
- Arora, V. K., and Coauthors, 2013: Carbon–concentration and carbon–climate feedbacks in CMIP5 Earth system models. J. Climate, 26, 5289–5314, https://doi.org/10.1175/JCLI-D-12-00494.1.
- —, and Coauthors, 2019: Carbon-concentration and carbonclimate feedbacks in CMIP6 models, and their comparison to CMIP5 models. *Biogeosci. Discuss.*, https://doi.org/10.5194/ bg-2019-473.
- Bala, G., K. Caldeira, A. Mirin, M. Wickett, C. Delire, and T. J. Phillips, 2006: Biogeophysical effects of CO₂ fertilization on global climate. *Tellus*, 58B, 620–627, https://doi.org/10.1111/ j.1600-0889.2006.00210.x.
- Ball, J. T., I. E. Woodrow, and J. A. Berry, 1987: A model predicting stomatal conductance and its contribution to the

- control of photosynthesis under different environmental conditions. *Progress in Photosynthesis Research*, J. Biggins, Ed., Springer, 221–224.
- Betts, R. A., 2000: Offset of the potential carbon sink from boreal forestation by decreases in surface albedo. *Nature*, **408**, 187–190, https://doi.org/10.1038/35041545.
 - —, P. M. Cox, S. E. Lee, and F. I. Woodward, 1997: Contrasting physiological and structural vegetation feedbacks in climate change simulations. *Nature*, 387, 796–799, https://doi.org/10.1038/42924.
- ——, and Coauthors, 2007: Projected increase in continental runoff due to plant responses to increasing carbon dioxide. *Nature*, **448**, 1037–1041, https://doi.org/10.1038/nature06045.
- Bonan, G. B., 2008: Forests and climate change: Forcings, feed-backs, and the climate benefits of forests. *Science*, 320, 1444–1449, https://doi.org/10.1126/science.1155121.
- Bony, S., and Coauthors, 2006: How well do we understand and evaluate climate change feedback processes? *J. Climate*, **19**, 3445–3482, https://doi.org/10.1175/JCLI3819.1.
- Boucher, O., A. Jones, and R. A. Betts, 2009: Climate response to the physiological impact of carbon dioxide on plants in the Met Office Unified Model HadCM3. *Climate Dyn.*, **32**, 237–249, https://doi.org/10.1007/s00382-008-0459-6.
- —, and Coauthors, 2013: Clouds and aerosols. *Climatic Change* 2013: The Physical Science Basis, T.F. Stocker et al., Eds., Cambridge University Press, 571–657.
- Bounoua, L., and Coauthors, 1999: Interactions between vegetation and climate: Radiative and physiological effects of doubled atmospheric CO₂. *J. Climate*, **12**, 309–324, https://doi.org/10.1175/1520-0442(1999)012<0309:IBVACR>2.0.CO;2.
- Byrne, M. P., and P. A. O'Gorman, 2016: Understanding decreases in land relative humidity with global warming: Conceptual model and GCM simulations. *J. Climate*, **29**, 9045–9061, https://doi.org/10.1175/JCLI-D-16-0351.1.
- —, and —, 2018: Trends in continental temperature and humidity directly linked to ocean warming. *Proc. Natl. Acad. Sci. USA*, **115**, 4863–4868, https://doi.org/10.1073/pnas.1722312115.
- Cao, L., G. Bala, K. Caldeira, R. Nemani, and G. Ban-Weiss, 2009: Climate response to physiological forcing of carbon dioxide simulated by the coupled Community Atmosphere Model (CAM3.1) and Community Land Model (CLM3.0). Geophys. Res. Lett., 36, L10402, https://doi.org/10.1029/2009GL037724.
- —, —, —, and —, 2010: Importance of carbon dioxide physiological forcing to future climate change. *Proc. Natl. Acad. Sci. USA*, **107**, 9513–9518, https://doi.org/10.1073/pnas.0913000107.
- Chadwick, R., H. Douville, and C. B. Skinner, 2017: Timeslice experiments for understanding regional climate projections: Applications to the tropical hydrological cycle and European winter circulation. *Climate Dyn.*, **49**, 3011–3029, https://doi.org/10.1007/s00382-016-3488-6.
- —, D. Ackerley, T. Ogura, and D. Dommenget, 2019: Separating the influences of land warming, the direct CO₂ effect, the plant physiological effect, and SST warming on regional precipitation changes. *J. Geophys. Res. Atmos.*, **124**, 624–640, https:// doi.org/10.1029/2018JD029423.
- Collatz, G. J., L. Bounoua, S. O. Los, D. A. Randall, I. Y. Fung, and P. J. Sellers, 2000: A mechanism for the influence of vegetation on the response of the diurnal temperature range to changing climate. *Geophys. Res. Lett.*, 27, 3381–3384, https://doi.org/ 10.1029/1999GL010947.
- Cox, P. M., R. A. Betts, C. B. Bunton, R. L. H. Essery, P. R. Rowntree, and J. Smith, 1999: The impact of new land surface

physics on the GCM simulation of climate and climate sensitivity. Climate Dyn., 15, 183-203, https://doi.org/10.1007/ s003820050276.

JOURNAL OF CLIMATE

- de Arellano, J. V.-G., C. C. van Heerwaarden, and J. Lelieveld, 2012: Modelled suppression of boundary-layer clouds by plants in a CO₂-rich atmosphere. Nat. Geosci., 5, 701-704, https://doi.org/10.1038/ngeo1554.
- De Kauwe, M. G., and Coauthors, 2013: Forest water use and water use efficiency at elevated CO2: A model-data intercomparison at two contrasting temperate forest FACE sites. Global Change Biol., 19, 1759-1779, https://doi.org/10.1111/gcb.12164.
- Deser, C., and Coauthors, 2020: Insights from Earth system model initial-condition large ensembles and future prospects. Nat. Climate Change, 10, 277-286, https://doi.org/10.1038/s41558-020-0731-2.
- Devaraju, N., G. Bala, and A. Modak, 2015: Effects of large-scale deforestation on precipitation in the monsoon regions: Remote versus local effects. Proc. Natl. Acad. Sci. USA, 112, 3257-3262, https://doi.org/10.1073/pnas.1423439112.
- -, N. de Noblet-Ducoudré, B. Quesada, and G. Bala, 2018: Quantifying the relative importance of direct and indirect biophysical effects of deforestation on surface temperature and teleconnections. J. Climate, 31, 3811–3829, https://doi.org/ 10.1175/JCLI-D-17-0563.1.
- Diffenbaugh, N. S., M. A. Snyder, and L. C. Sloan, 2004: Could CO2-induced land-cover feedbacks alter near-shore upwelling regimes? Proc. Natl. Acad. Sci. USA, 101, 27-32, https:// doi.org/10.1073/pnas.0305746101.
- Dong, B., J. M. Gregory, and R. T. Sutton, 2009: Understanding land-sea warming contrast in response to increasing greenhouse gases. Part I: Transient adjustment. J. Climate, 22, 3079-3097, https://doi.org/10.1175/2009JCLI2652.1.
- Donohue, R. J., M. L. Roderick, T. R. McVicar, and G. D. Farquhar, 2013: Impact of CO₂ fertilization on maximum foliage cover across the globe's warm, arid environments. Geophys. Res. Lett., 40, 3031-3035, https://doi.org/10.1002/grl.50563.
- Doutriaux-Boucher, M., M. J. Webb, J. M. Gregory, and O. Boucher, 2009: Carbon dioxide induced stomatal closure increases radiative forcing via a rapid reduction in low cloud. Geophys. Res. Lett., 36, L02703, https://doi.org/10.1029/2008GL036273.
- Douville, H., S. Planton, J.-F. Royer, D. B. Stephenson, S. Tyteca, L. Kergoat, S. Lafont, and R. A. Betts, 2000: Importance of vegetation feedbacks in doubled-CO2 climate experiments. J. Geophys. Res. Atmos., 105, 14841–14861, https://doi.org/ 10.1029/1999JD901086.
- Field, C. B., R. B. Jackson, and H. A. Mooney, 1995: Stomatal responses to increased CO₂: Implications from the plant to the global scale. Plant Cell Environ., 18, 1214-1225, https:// doi.org/10.1111/j.1365-3040.1995.tb00630.x.
- Fisher, R. A., and Coauthors, 2019: Parametric controls on vegetation responses to biogeochemical forcing in the CLM5. J. Adv. Model. Earth Syst., 11, 2879–2895, https://doi.org/ 10.1029/2+019MS001609.
- Flynn, C. M., and T. Mauritsen, 2020: On the climate sensitivity and historical warming evolution in recent coupled model ensembles. Atmos. Chem. Phys., 20, 7829-7842, https://doi.org/ 10.5194/acp-20-7829-2020.
- Friedlingstein, P., and Coauthors, 2006: Climate-carbon cycle feedback analysis: Results from the C4MIP model intercomparison. J. Climate, 19, 3337–3353, https://doi.org/10.1175/JCLI3800.1.
- Geoffroy, O., D. Saint-Martin, and A. Ribes, 2012: Quantifying the sources of spread in climate change experiments. Geophys. Res. Lett., 39, L24703, https://doi.org/10.1029/2012GL054172.

- Gettelman, A., and Coauthors, 2019: High climate sensitivity in the Community Earth System Model version 2 (CESM2). Geophys. Res. Lett., 46, 8329-8337, https://doi.org/10.1029/ 2019GL083978.
- Golaz, J.-C., and Coauthors, 2019: The DOE E3SM coupled model version 1: Overview and evaluation at standard resolution. J. Adv. Model. Earth Syst., 11, 2089-2129, https://doi.org/ 10.1029/2018MS001603.
- Green, J. K., A. G. Konings, S. H. Alemohammad, J. Berry, D. Entekhabi, J. Kolassa, J.-E. Lee, and P. Gentine, 2017: Regionally strong feedbacks between the atmosphere and terrestrial biosphere. Nat. Geosci., 10, 410-414, https://doi.org/ 10.1038/ngeo2957.
- Gregory, J. M., and P. M. Forster, 2008: Transient climate response estimated from radiative forcing and observed temperature change. J. Geophys. Res., 113, D23105, https://doi.org/10.1029/ 2008JD010405.
- , and Coauthors, 2004: A new method for diagnosing radiative forcing and climate sensitivity. Geophys. Res. Lett., 31, L03205, https://doi.org/10.1029/2003GL018747.
- -, T. Andrews, and P. Good, 2015: The inconstancy of the transient climate response parameter under increasing CO₂. Philos. Trans. Roy. Soc., **373**, 20140417, https:// doi.org/10.1098/rsta.2014.0417.
- Grose, M. R., J. Gregory, R. Colman, and T. Andrews, 2018: What climate sensitivity index is most useful for projections? Geophys. Res. Lett., 45, 1559-1566, https://doi.org/10.1002/ 2017GL075742.
- Hansen, J., and Coauthors, 2005: Efficacy of climate forcings. J. Geophys. Res., 110, D18104, https://doi.org/10.1029/ 2005JD005776.
- Hense, I., I. Stemmler, and S. Sonntag, 2017: Ideas and perspectives: Climate-relevant marine biologically driven mechanisms in Earth system models. Biogeosciences, 14, 403-413, https://doi.org/10.5194/bg-14-403-2017.
- Hungate, B. A., M. Reichstein, P. Dijkstra, D. Johnson, G. Hymus, J. D. Tenhunen, C. R. Hinkle, and B. G. Drake, 2002: Evapotranspiration and soil water content in a scrub-oak woodland under carbon dioxide enrichment. Global Change Biol., 8, 289-298, https://doi.org/10.1046/j.1365-2486.2002.00468.x.
- Jones, C. D., and Coauthors, 2016: C4MIP-The Coupled Climate-Carbon Cycle Model Intercomparison Project: Experimental protocol for CMIP6. Geosci. Model Dev., 9, 2853-2880, https://doi.org/10.5194/gmd-9-2853-2016.
- Joshi, M. M., J. M. Gregory, M. J. Webb, D. M. H. Sexton, and T. C. Johns, 2008: Mechanisms for the land/sea warming contrast exhibited by simulations of climate change. Climate Dyn., 30, 455-465, https://doi.org/10.1007/s00382-007-0306-1.
- Keenan, T. F. and W. J. Riley, 2018: Greening of the land surface in the world's cold regions consistent with recent warming. Nat. Climate Change, 8, 825-828, https://doi.org/10.1038/s41558-018-0258-v.
- Kooperman, G. J., Y. Chen, F. M. Hoffman, C. D. Koven, K. Lindsay, M. S. Pritchard, A. L. S. Swann, and J. T. Randerson, 2018a: Forest response to rising CO2 drives zonally asymmetric rainfall change over tropical land. Nat. Climate Change, 8, 434-440, https://doi.org/10.1038/s41558-018-0144-7.
- , M. D. Fowler, F. M. Hoffman, C. D. Koven, K. Lindsay, M. S. Pritchard, A. L. S. Swann, and J. T. Randerson, 2018b: Plant physiological responses to rising CO₂ modify simulated daily runoff intensity with implications for global-scale flood risk assessment. Geophys. Res. Lett., 45, 12457-12466, https:// doi.org/10.1029/2018GL079901.

- Laguë, M. M., and A. L. S. Swann, 2016: Progressive midlatitude afforestation: Impacts on clouds, global energy transport, and precipitation. *J. Climate*, 29, 5561–5573, https://doi.org/ 10.1175/JCLI-D-15-0748.1.
- ——, G. B. Bonan, and A. L. S. Swann, 2019: Separating the impact of individual land surface properties on the terrestrial surface energy budget in both the coupled and uncoupled landatmosphere system. J. Climate, 32, 5725–5744, https://doi.org/ 10.1175/JCLI-D-18-0812.1.
- Langenbrunner, B., M. S. Pritchard, G. J. Kooperman, and J. T. Randerson, 2019: Why does Amazon precipitation decrease when tropical forests respond to increasing CO₂? *Earth's Future*, **7**, 450–468, https://doi.org/10.1029/2018EF001026.
- Leakey, A. D. B., E. A. Ainsworth, C. J. Bernacchi, A. Rogers, S. P. Long, and D. R. Ort, 2009: Elevated CO₂ effects on plant carbon, nitrogen, and water relations: Six important lessons from FACE. J. Exp. Bot., 60, 2859–2876, https://doi.org/10.1093/jxb/erp096.
- Lemordant, L., and P. Gentine, 2019: Vegetation response to rising CO₂ impacts extreme temperatures. *Geophys. Res. Lett.*, 46, 1383–1392, https://doi.org/10.1029/2018GL080238.
- —, —, M. Stéfanon, P. Drobinski, and S. Fatichi, 2016: Modification of land-atmosphere interactions by CO₂ effects: Implications for summer dryness and heat wave amplitude. *Geophys. Res. Lett.*, 43, 10 240–10 248, https://doi.org/10.1002/2016GL069896.
- —, —, A. S. Swann, B. I. Cook, and J. Scheff, 2018: Critical impact of vegetation physiology on the continental hydrologic cycle in response to increasing CO₂. *Proc. Natl. Acad. Sci. USA*, 115, 4093–4098, https://doi.org/10.1073/pnas.1720712115.
- Levis, S., J. A. Foley, and D. Pollard, 2000: Large-scale vegetation feedbacks on a doubled CO₂ climate. *J. Climate*, 13, 1313–1325, https://doi.org/10.1175/1520-0442(2000)013<1313: LSVFOA>2.0.CO;2.
- Lian, X., and Coauthors, 2018: Partitioning global land evapotranspiration using CMIP5 models constrained by observations. *Nat. Climate Change*, 8, 640–646, https://doi.org/10.1038/s41558-018-0207-9.
- Lin, Y.-S., and Coauthors, 2015: Optimal stomatal behaviour around the world. *Nat. Climate Change*, 5, 459–464, https:// doi.org/10.1038/nclimate2550.
- Lutsko, N. J., and M. Popp, 2019: Probing the sources of uncertainty in transient warming on different timescales. Geophys. Res. Lett., 46, 11367–11377, https://doi.org/10.1029/2019GL084018.
- Mahowald, N., F. Lo, Y. Zheng, L. Harrison, C. Funk, D. Lombardozzi, and C. Goodale, 2016: Projections of leaf area index in Earth system models. *Earth Syst. Dyn.*, 7, 211– 229, https://doi.org/10.5194/esd-7-211-2016.
- Medlyn, B. E., and Coauthors, 2011: Reconciling the optimal and empirical approaches to modelling stomatal conductance. *Global Change Biol.*, **17**, 2134–2144, https://doi.org/10.1111/j.1365-2486.2010.02375.x.
- Norby, R. J., and D. R. Zak, 2011: Ecological lessons from free-air CO₂ enrichment (FACE) experiments. *Annu. Rev. Ecol. Evol. Syst.*, **42**, 181–203, https://doi.org/10.1146/annurevecolsys-102209-144647.
- O'ishi, R., A. Abe-Ouchi, I. C. Prentice, and S. Sitch, 2009: Vegetation dynamics and plant CO₂ responses as positive feedbacks in a greenhouse world. *Geophys. Res. Lett.*, **36**, L11706, https://doi.org/10.1029/2009GL038217.
- Park, S.-W., J.-S. Kim, and J.-S. Kug, 2020: The intensification of Arctic warming as a result of CO₂ physiological forcing.

- Nat. Commun., 11, 2098, https://doi.org/10.1038/s41467-020-15924-3.
- Parsons, L. A., K. M. Brennan, R. C. Jnglin Wills, and C. Proistosescu, 2020: Magnitudes and spatial patterns of interdecadal temperature variability in CMIP6. *Geophys. Res. Lett.*, 47, e2019GL086588, https://doi.org/10.1029/ 2019GL086588.
- Piao, S., and Coauthors, 2013: Evaluation of terrestrial carbon cycle models for their response to climate variability and to CO₂ trends. *Global Change Biol.*, **19**, 2117–2132, https://doi.org/10.1111/gcb.12187.
- Pu, B., and R. E. Dickinson, 2012: Examining vegetation feed-backs on global warming in the Community Earth System Model. *J. Geophys. Res.*, 117, D20110, https://doi.org/10.1029/2012JD017623.
- Qian, H., R. Joseph, and N. Zeng, 2010: Enhanced terrestrial carbon uptake in the northern high latitudes in the 21st century from the Coupled Carbon Cycle Climate Model Intercomparison Project model projections. *Global Change Biol.*, 16, 641–656, https:// doi.org/10.1111/j.1365-2486.2009.01989.x.
- Richardson, T. B., and Coauthors, 2018: Carbon dioxide physiological forcing dominates projected eastern Amazonian drying. *Geophys. Res. Lett.*, 45, 2815–2825, https://doi.org/10.1002/2017GL076520.
- Roe, G., 2009: Feedbacks, timescales, and seeing red. *Annu. Rev. Earth Planet. Sci.*, **37**, 93–115, https://doi.org/10.1146/annurev.earth.061008.134734.
- Saint-Lu, M., R. Chadwick, F. H. Lambert, and M. Collins, 2019: Surface warming and atmospheric circulation dominate rainfall changes over tropical rainforests under global warming. *Geophys. Res. Lett.*, 46, 13 410–13 419, https://doi.org/10.1029/2019GL085295.
- Schimel, D., B. B. Stephens, and J. B. Fisher, 2015: Effect of increasing CO₂ on the terrestrial carbon cycle. *Proc. Natl. Acad. Sci. USA*, 112, 436–441, https://doi.org/10.1073/pnas.1407302112.
- Sellers, P. J., and Coauthors, 1996: Comparison of radiative and physiological effects of doubled atmospheric CO₂ on climate. *Science*, **271**, 1402–1406, https://doi.org/10.1126/science.271.5254.1402.
- Sherwood, S. C., S. Bony, O. Boucher, C. Bretherton, P. M. Forster, J. M. Gregory, and B. Stevens, 2015: Adjustments in the forcing-feedback framework for understanding climate change. *Bull. Amer. Meteor. Soc.*, 96, 217–228, https://doi.org/ 10.1175/BAMS-D-13-00167.1.
- Skinner, C. B., C. J. Poulsen, and J. S. Mankin, 2018: Amplification of heat extremes by plant CO₂ physiological forcing. *Nat. Commun.*, 9, 1094, https://doi.org/10.1038/s41467-018-03472-w.
- Smith, W. K., S. C. Reed, C. C. Cleveland, A. P. Ballantyne, W. R. L. Anderegg, W. R. Wieder, Y. Y. Liu, and S. W. Running, 2016: Large divergence of satellite and Earth system model estimates of global terrestrial CO₂ fertilization. *Nat. Climate Change*, 6, 306–310, https://doi.org/ 10.1038/nclimate2879.
- Swann, A. L. S., I. Y. Fung, and J. C. H. Chiang, 2012: Mid-latitude afforestation shifts general circulation and tropical precipitation. *Proc. Natl. Acad. Sci. USA*, **109**, 712–716, https://doi.org/10.1073/pnas.1116706108.
- ——, Y. Liu, and J. C. H. Chiang, 2014: Remote vegetation feedbacks and the mid-Holocene Green Sahara. *J. Climate*, 27, 4857–4870, https://doi.org/10.1175/JCLI-D-13-00690.1.
- —, F. M. Hoffman, C. D. Koven, and J. T. Randerson, 2016: Plant responses to increasing CO₂ reduce estimates of climate impacts on drought severity. *Proc. Natl. Acad. Sci. USA*, **113**, 10 019–10 024, https://doi.org/10.1073/pnas.1604581113.

- Tang, T., and Coauthors, 2019: Comparison of effective radiative forcing calculations using multiple methods, drivers, and models. *J. Geophys. Res. Atmos.*, 124, 4382–4394, https://doi.org/10.1029/ 2018JD030188.
- Vargas Zeppetello, L. R., A. Donohoe, and D. S. Battisti, 2019: Does surface temperature respond to or determine down-welling longwave radiation? *Geophys. Res. Lett.*, 46, 2781–2789, https://doi.org/10.1029/2019GL082220.
- Vial, J., J.-L. Dufresne, and S. Bony, 2013: On the interpretation of intermodel spread in CMIP5 climate sensitivity estimates. *Climate Dyn.*, 41, 3339–3362, https://doi.org/10.1007/s00382-013-1725-9.
- Vico, G., S. Manzoni, S. Palmroth, and G. Katul, 2011: Effects of stomatal delays on the economics of leaf gas exchange under

- intermittent light regimes. *New Phytol.*, **192**, 640–652, https://doi.org/10.1111/j.1469-8137.2011.03847.x.
- Webb, M. J., and Coauthors, 2017: The Cloud Feedback Model Intercomparison Project (CFMIP) contribution to CMIP6. Geosci. Model Dev., 10, 359–384, https://doi.org/10.5194/gmd-10-359-2017.
- Wolz, K. J., T. M. Wertin, M. Abordo, D. Wang, and A. D. B. Leakey, 2017: Diversity in stomatal function is integral to modelling plant carbon and water fluxes. *Nat. Ecol. Evol.*, 1, 1292–1298, https://doi.org/10.1038/s41559-017-0238-z.
- Xu, X., W. J. Riley, C. D. Koven, G. Jia, and X. Zhang, 2020: Earlier leaf-out warms air in the north. *Nat. Climate Change*, 10, 370–375, https://doi.org/10.1038/s41558-020-0713-4.